Trailing Edge Design to Reduce the Wake Mixing Loss of Low Pressure Turbine Airfoil

Juo Furukawa[1] , Masaaki Hamabe, Yasuhiro Okamura and Kenichi Funazaki[2]

[1] Aerodynamic Technology Gr. Advanced Technology Deps., Research & Engineering Division,
Aero-Engine & Space Operations, IHI corp.
229. Tonogaya, Mizuho-machi, Nishitama-gun, Tokyo 190-1297, Japan
[2] Departments of Mechanical Engineering, Iwate University, Morioka, Japan

ABSTRACT

The trailing edge of the Low Pressure Turbine (LPT) airfoil needs to have a certain amount of thickness due to the constraints of castability or vibrational strength. This contributes to the mixing loss of wake from the trailing edge. In order to achieve a further improvement of LPT performance, the authors had invented the trailing edge profile to reduce the wake mixing loss while maintaining the castability and vibrational characteristics and demonstrated an effect using low speed cascade test.

This paper represents the effect of the new trailing edge profile on loss reduction. In order to improvement of the total pressure loss, a high speed rotational test rig is demonstrated. The experiment simulates LPT of modern aero engines. The mechanisms of the loss reduction are discussed by using result from low speed cascade experiment conducted in Iwate University.

NUMENCLATURE

C	: true chord length
Cx	: axial chord length
C_{pb}	: base pressure coefficient
f_w	: wake passing frequency
Mn	: normalized isentropic Mach number distribution on surface of airfoil
n	: pitch-wise coordinate
$p_{t,in,ave}$	: turbine inlet mass-averaged total pressure
$p_{t,ex}$	: turbine exit local total pressure
$p_{t,ex,ave}$	: turbine exit mass-averaged total pressure
$p_{s,ex}$	: turbine exit local static pressure
$p_{s,ex,ave}$	: turbine exit mass-averaged static pressure
p_b	: base pressure
Re	: Reynolds number based on actual chord length and exit velocity
St	: Strouhal number (non-dimensional wake passing frequency $= f_w C/V_{ex,ave}$
s	: airfoil surface distance from leading edge
t	: trailing edge thickness
u	: magnitude of velocity
U	: free stream velocity
V_{in} $V_{ex,ave}$	: turbine blade inlet, averaged exit velocity
w	: length of throat
x	: axial coordinate
ζ	: estimated total pressure loss coefficient
$\Delta\zeta$	: total pressure loss reduction rate of PTE compared with BTE
ζ_d	: Denton's total pressure loss coefficient [2]
δ^*	: displacement thickness of boundary layer
θ	: momentum thickness of boundary layer
ρ	: density of fluid

Abbreviation

BTE	: Base type TE
FWHM	: Full Width at Half Maximum
HSR	: High Speed Rotating rig
LE	: Leading Edge
LPT	: Low Pressure Turbine
LSC	: Low Speed Cascade test
TE	: Trailing Edge
PS	: Pressure Surface
PTE	: Profiled TE
SS	: Suction Surface

INTRODUCTON

In design of modern civil jet engines, there is great effort in increasing the performance. Also the aerodynamic loss reduction of order of 1% is necessary. Therefore, a lot of study of loss reduction is published. The loss caused at LPT is separated into three types: "profile loss", "endwall loss", "leakage loss" categorized by Denton [1]. The profile loss is generated in the blade boundary layers well away from the end walls and it depends on boundary layer thickness comparing with length of throat, base pressure around the TE and blockage ratio (TE thickness/throat). Mee et al [2] showed that the majority of two dimensional blade loss comes from trailing edge (TE) loss. They shows that the two boundary layer mixings with different growth rate and expansion of the flow path at TE. Therefore the turbine blade loss is influenced by the TE thickness. This means the thinner blade comparing with length of throat has more advantage to reduce the losses and it is need to be as thin as possible. However the turbine blade is made thinner towards the TE, manufacturing of the blade becomes difficult because of the misrun of melted metal and complexity of machining. Moreover, the minimum TE thickness is the same extent regardless of size of a jet engine. This is especially true for the small engine that has shorter throat because the effect of the blockage ratio is relatively larger than that of large engine.

We have proposed the locally thin airfoil that named "profiled trailing edge" (PTE). The improvement of performance has been confirmed by the low-speed cascade equipment at Iwate University. The results of the cascade experiments showed a reduction of 10 % in the PTE's total pressure loss coefficient when compared to the general TE shape under high Reynolds conditions [3]. Funazaki & Okamura [4] also showed that enhancing the turbulence by combing PTE and step on the suction surface at Re = 4.0 to 17×10^4 is able to reduce the LPT profile loss. Recirculation region is observed at the TE in their study and it was considered that the recirculation region is the one of the factor to reduce the loss. Also the some studies by changing/adding to TE to improve the LPT performance, some of configurations were studied (gurney flap[5] and jet flap[6]). Chao et al [7] showed that locally thinned the TE of on

ISBN978-4-89111-008-6
Copyright© 2015 Gas Turbine Society of Japan

the pressure surface (PS) decreases the mix loss by increasing the base pressure.

In this paper, the loss reduction is proposed by using developed new trailing edge configuration. In order to demonstrate wake mixing loss improvement, high speed rotational rig testing that simulated real world operating conditions, was conducted. The loss reduction mechanism is considered by comparing results from low speed cascade experiment at Iwate University.

EXPERIMENTAL METHOD

Low speed cascade experiment (Iwate University)

An overview of the cascade experiment with wake generator is shown in Fig. 1 and the experimental condition is shown in Table 1. Total seven airfoils including two special airfoils which contains static pressure hole are aligned (Blade 3 and 4 in Fig. 1). There are cylinders in front of testing airfoil which has 3-milimeter in diameter. The cylinders are fixed on timing belt. When the flow flows into the test facility, the cylinders generate Von' Karman vortex (wake) and the wake is fluid to airfoil intermittently. Then it can simulate the incoming wake interaction. In order to characterize the flow field, the Strouhal number St is chosen. The details of equipment and measurement methods are referenced from [3,4].

The tested airfoil configuration is shown in Fig. 2. The solid-line in Fig. 2 is resulting from profiled TE (PTE), the other is original airfoil (base type TE: BTE). As is seen in Fig. 2, the thickness of PTE around the TE is smaller than that of BTE.

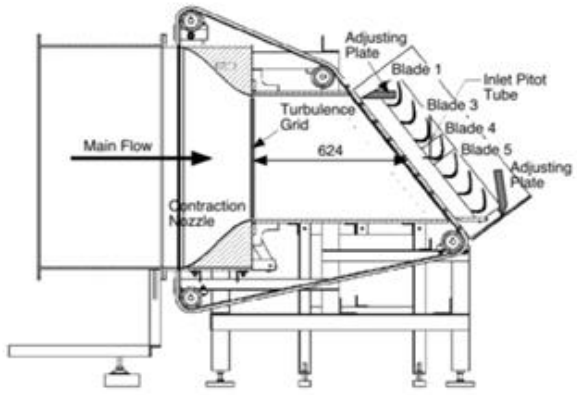

Fig. 1: Test apparatus of low speed cascade experiment [4].

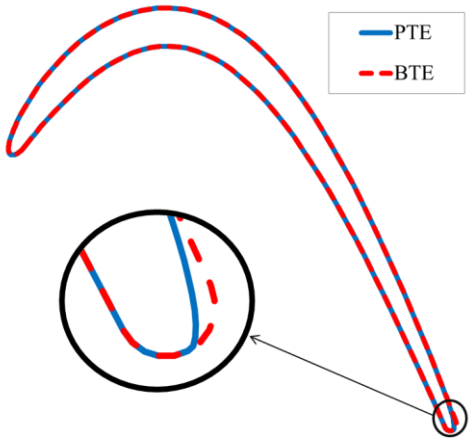

Fig. 2: Cross-sectional geometry of two airfoils tested at Iwate University for low speed cascade experiment, enlarged TE configuration (circled area).

Table 1: Combination of Reynolds (Re) number and Strauhal (St) number conducted with LSC at Iwate University

Re	St = 0.0	0.4	0.8	1.2
4.0×10^4	○	○	○	○
5.7×10^4	○	○	○	○
1.0×10^5	○	○	○	×
1.7×10^5	○	○	×	×

Before describing about HSR, we want to discuss the the results from the LSC. In order to estimate the effects of PTE, the LSC is conducted under the condition with/without moving cylinders and it has been shown by Okamura et al[4]. Fig. 3 shows the mass-averaged total pressure loss coefficient along to pitch direction of the BTE and the PTE. In calculation of mass averaged value, the following definition of total pressure coefficient ζ is used.

$$\zeta = \frac{p_{t,ex} - p_{t,in,ave}}{p_{t,ex,ave} - p_{s,ex,ave}}. \quad (1)$$

In the calculation of Eq. (1), measured total and static pressure, $p_{t,ex}$ and $p_{s,ex}$ at turbine exit (15%Cx far from TE) and measured inlet total pressure $p_{t,in}$ are used and the subscript "ave" indicates the mass-flow average. These values are averaged by sampling time and. The test conditions of Re are setted to 4.0×10^4, 5.7×10^4, 1.0×10^5 and 1.7×10^5 as shown in Table 1. In Fig. 3, the blanked and filled marker indicate with/without wake generator (that means St = 0.0 and 0.8). As shown in Fig. 3, it can be seen that the improvement of the PTE is depend on Reynolds number for the condition of St = 0.0. According to the Okamura [3], the large separation around TE is observed at low Reynolds number by using the boundary layer measurement. And the improvement is obtained over Re = 1.0×10^5 with St = 0.0. In general, increasing Reynolds condition, boundary layer thickness is decreasing and the separation is delayed because of the turbulent enhancement. The improvement of the PTE is 6 % at the Re = 1.7×10^5. However the reduction of the total pressure loss coefficient is observed at low Reynolds number and high Strouhal number. It is expected that the interaction between incoming wake and boundary layer prevents the boundary layer separation that occurs at low Re number and no incoming wake condition. Therefore, it can be expected that further improvement can be obtained in the conditions which are close to the actual conditions.

In order to elucidate the total loss reduction, the velocity profiles are also measured at downstream (104-180%Cx) as shown in Fig. 4. In Fig. 4, the contours are normalized by the free stream

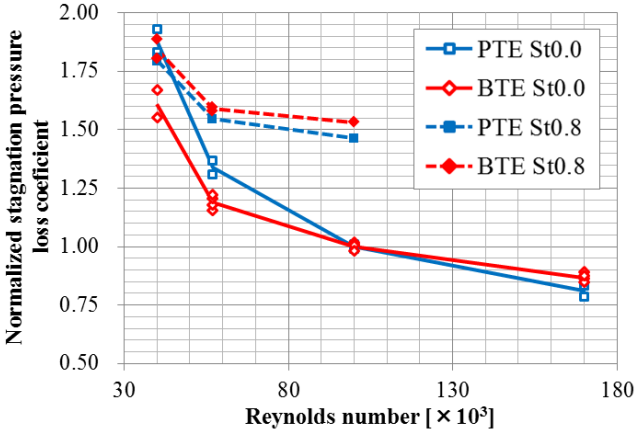

Fig. 3: Mass averaged total pressure loss coefficient distribution of the BTE and the PTE airfoil for Re=4.0×10^4 to 1.7×10^5 with St=0.0 and 0.8.

velocity. Note that the origin of the velocity distribution locates the TE. As seen in Fig. 4, the contour lines are narrower as far from TE for the condition PTE. It indicates that the area of the high speed region of PTE is larger than that of the BTE. Accordingly the smaller the velocity deficit region, the reduction of total pressure loss coefficient in turn decreasing toward to downstream. For the visualization of the velocity deficit effect, full width at half maximum (FWHM) and the maximum value of the velocity deficit are introduced and it is plotted in Fig. 5. Note that the Fig. 5 is normalized by the value at 104%*Cx* for BTE. Comparing the FWHM of the PTE and the BTE, there is no obvious difference between BTE and PTE near the TE. However the trend curves of the FWHM and velocity deficit values are different over the position of 115% *Cx*. In the region over 115% *Cx*, the FWHM is increasing rapidly and the velocity deficit becomes smaller than one of the BTE. It shows that the PTE improves the mixing at downstream. It can be considered that the diffusion and velocity deficit of the PTE is smaller than that of the BTE. It indicates that PTE has a velocity recovery effect and also has the effect to enhance the diffusion in the wake.

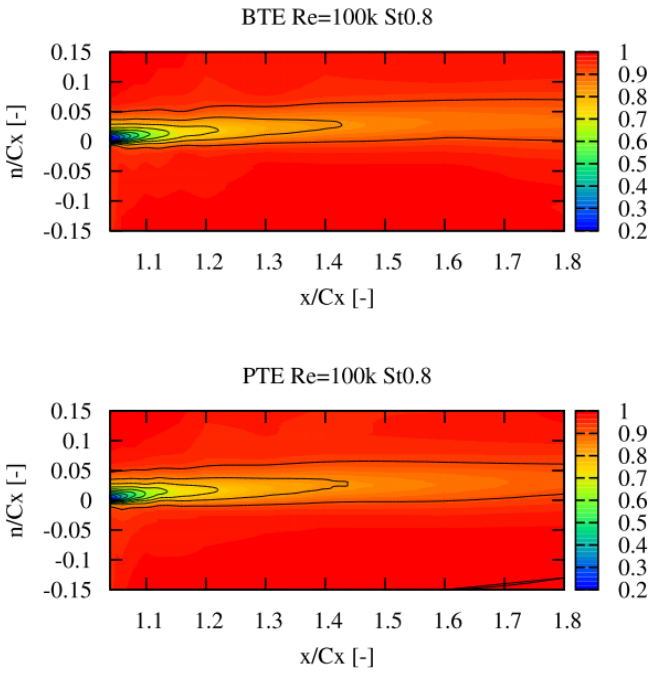

Fig. 4: Normalized velocity contours at behind of the BTE and the PTE airfoils under Re=1.0×10^5 and St = 0.8

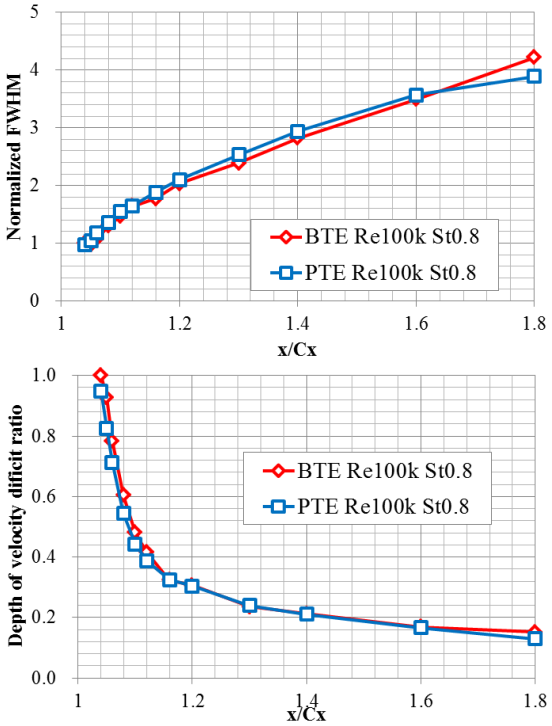

Fig. 5: Full width at half maximum (FWHM) and velocity deficit peak distribution at downstream of BTE and PTE arifoils.

High Speed Rotational rig

An overview of the 1.5-stage high-speed rotational rig is shown in Fig. 6. The test rig was designed by IHI and it simulates LPT of modern civil engines. Test was carried out relatively; the effect of using PTE is evaluated by replacing the basic type airfoil (BTE) to the airfoil of the PTE at 2nd stage nozzle (2N). In order to measure the performance of 2N, traversed measurement is conducted at upstream and downstream of 2N. Traverse fine movement device is able to move arbitrarily changing in the span direction. The test condition is shown in Table 2.

Tested airfoil configuration is shown in Fig.7. Comparing with two tested airfoil, it can be seen that the TE at suction surface for the PTE airfoil is shaved. The decision method for TE between Iwate University's airfoil and tested airfoil is same. The detail of configuration is not made clear because of a special permission.

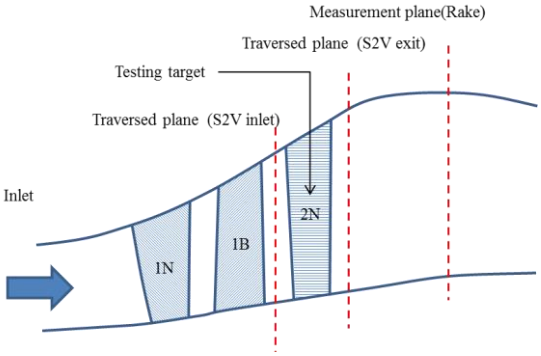

Fig. 6: Schematics of 1.5-stage high speed rotational rig. The dashed lines denote the measurement planes.

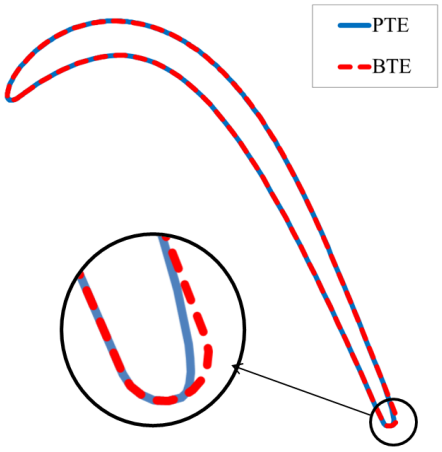

Fig. 7: Cross-sectional geometry of the two types of tested airfoils for high speed rotating rig. Bottom left circled picture denotes enlarged TE configuration

Table 2: Summary of test condition of rotating rig at 2N exit

Parameter	Value
Reynolds number, Re	1.8×10^5
Strauhal number, St	1.56
Turbine exit Mach number@50%Span	0.47

RESULTS

Figure 8 shows the total pressure coefficient, ζ distribution under the Re = 1.7×10^5, St = 0.4 condition at LSC. Also Figure 9 shows the total pressure coefficient distribution resulting from the HSR. Note that the distributions of total pressure loss coefficient are normalized by mean peak value of the BTE for each experiment and the measured position is normalized by geometrical pitch length. The geometrical pitch length is defined as circular length divided by the number of airfoils. Because of same cross sectional configuration for cascade experiment, the 50% span is measured. However for HSR, the difference of circumferential velocity at rotational experiment, the cross sectional configuration is gradually changed. In Fig. 9, the measured total pressure at 50% span on designed stream line is used. From these results, it can be seen that the wake-width of the PTEs are the same as one of the BTEs. However, the maximum total pressure loss coefficient of the PTEs is smaller than that of the BTEs. Accordingly, it is expected that the integrated total pressure loss coefficient is improved by using the PTE. In order to show influence of PTE on total pressure loss coefficient, ensemble average of mass averaged total pressure coefficients are shown in Table 3. When calculating the mean value, the test results from the 3 times conducted tests were used. For low speed cascade experiment, the improvement of loss coefficient by using PTE is 5.4%, and is 9.7% for the high speed rotating rig. Thus, the total pressure loss coefficient for high speed rig condition is 1.7 times larger than that for the low speed cascade experiment. Therefore, the influence of the total pressure loss coefficient on the PTE for the high speed rotating rig is larger than that for low speed cascade experiment.

Table 3: Reduction rate of integrated loss coefficient by using PTEs

Experiment	Integrated loss reduction rate
Low speed cascade	5.4 %
High speed rotating rig	9.7 %

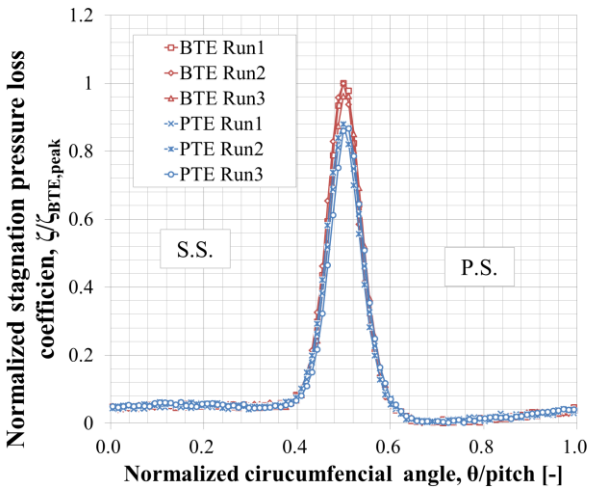

Fig. 8 Normalized total loss distribution of the BTE (red line) and the PTE (blue line) airfoils tested on low speed rotating rig at Re=1.7×10^5 and St=0.4.

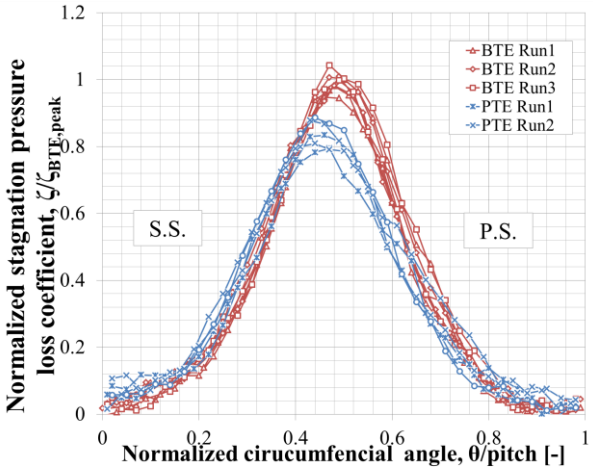

Fig. 9: Normalized total loss distribution of the BTE (red line) and the PTE (blue line) airfoil tested on the high speed rotating rig.

DISCUSSION

The difference between low speed cascade experiment and the high speed rotational rig experiment are test condition and configuration of airfoils. The difference of test condition is Re-number, St-number, Mach number and the differences of configuration of airfoils are TE thickness limited by mechanical process and design point. In order to breakdown the influence of the PTE on parameters, the Denton's loss model [1] shown as Eq. (2) was used.

$$\zeta_d = -C_{pb}\frac{t}{w} + \frac{2\theta}{w} + \left(\frac{\delta^* + t}{w}\right)^2 \quad (2)$$

Here ζ_d shows the total pressure loss coefficient, w is the length of throat, t is TE thickness. θ and δ^* is the momentum and displacement thickness of boundary layer respectively. The base pressure coefficient C_{pb} is defined as following.

$$C_{pb} = \frac{p_b - p_{s,ex}}{1/2\,\rho\, V_{ex}^2} \quad (3)$$

In Eq. (3), subscript *b* and *ex* indicate the position of the base region and the turbine blade exit. First term of Eq. (2) shows the effect of base pressure, second term of Eq. (2) is the effect of momentum thickness, and third term of Eq. (2) is the effect of blockage.

Effect of blockage

The one of the differences between the low speed cascade experiment and high speed rotational rig is TE blockage (t/w). TE blockage is defined as a ratio of TE thickness to the length of the throat. In order to realize modern LPT test conditions, the chord length tends to small as shown in introduction. However, the minimum TE thickness is limited by mechanical processing. Therefore the TE blockage for the high speed rotating rig is relatively larger than that of cascade experiment. In this study, the TE blockages of airfoil used in the high speed rotating rig is 1.5 times larger than those in the airfoils used in the low speed cascade experiment.

In order to estimate the effect of TE blockage, following 4 patterns of Eq. (2) were calculated. The calculating patterns are shown in Table 4. Firstly, by comparing patterns (A) and (B), the loss reduction for the low speed cascade experiment, ($\Delta\zeta_{12}$) is estimated. Secondly, by comparing patterns (C) and (D), the loss reduction for the high speed rotating rig, ($\Delta\zeta_{34}$) was estimated. Finally, loss reduction for low speed cascade and high speed rotating rig is compared. Note that the calculations of base pressure coefficients are assumed as -0.13 respect. The calculated loss reduction rate is

shown in Table 5. However the boundary layer thickness cannot measure in our experiment. Therefore, the CFD results are compared. In order to estimate the 3rd term of Eq. (2), the velocity deficit is calculated. The reduction rates of the width of velocity deficit are 4% for LSC and 8% for HSR. Using this reduction rate, the loss reduction of 3rd term calculated from Eq. (2) is 4% of the PTE comparing with the BTE for LSC, and is 6% for HSR. Therefore the reduction of total pressure loss coefficient by using the PTE for HSR is 2% smaller than that of LSCs.

Table 4: Comparing patterns for estimating the effect on TE blockage

Pattern	TE thickness	Boundary layer thickness
(A)	BTE for LSC	Measured at LSC conditions under $Re=1.0\times10^5$, St=0.8 of BTE
(B)	PTE for LSC	Measured at LSC conditions under $Re=1.0\times10^5$, St=0.8 of BTE
(C)	BTE for HSR	Assuming the ratio of boundary layer thickness to length of throat is same as pattern (A)
(D)	PTE for HSR	Assuming the ratio of boundary layer thickness to length of throat is same as pattern (A)

Table 5: The reduction rate of Denton loss (Eq. 2) found by using the PTE for each TE blockage

	LSC	HSR	$\Delta\zeta$
$\Delta\zeta$ of 1st term	4%	6 %	2%
$\Delta\zeta$ of 2nd term	0 %	0 %	0%
$\Delta\zeta$ of 3rd term	6 %	10%	4%
Total difference	10%	16 %	6%

Effect of base pressure

In order to estimate the contribution of base pressure on loss reduction, the CFD is conducted. In order to simulate the separated flow transition, the SST γ-Re_Θ model based on the coupling of the SST k-ω transport equation is used. The model constants are referenced from Menter et al.[8]. Fig. 10 shows the difference of the base pressure coefficient around the TE because the estimation of total pressure loss coefficient by using Eq. (2) is only considered the difference. The base pressure distribution plotted as the function of surface length and the origin is located at TE. Note that the surface length from TE is normalized by the half length of TE circumference. In both figure, red line indicates the BTEs, and blue line indicates the PTEs result. As seen in Fig. 10, base pressure coefficients of the PTE are larger than that of the BTE for both calculations. The averaged difference of on the base pressure coefficient is 0.03 for the LSC and 0.05 for the HSR. Note that, the difference of base pressure is only considered although the 1st term of Eq (2) indicates base pressure coefficient depends on TE blockage. Using the estimated value, the loss reduction rate is 4% for the LSC and 6% for HSR. Comparing the loss reduction rate of the LSC and that of the HSR, the ratio of total pressure loss coefficient of the LSC and the HSR is 2%. Also note that it has spread the flow passage for the HSR as shown in Fig. 6. The effect of divergence and deceleration at downstream is included in this discussion.

Effect of incoming wake on loss

In order to estimate the influence of incoming wake on the cascade loss, we discuss the experimental results from LSC. Fig. 11 shows results from the LSC under the Re = 1.0×10^5 and 1.7×10^5 with various St-number. The values in Fig. 11 are normalized by total pressure loss coefficient of BTE under $Re=1.0\times10^5$ and St = 0.0. For no-wake condition, the loss coefficient decreases with increasing the Re-number. However for high St-number condition, the loss reduction rate of PTE is about 6% from BTE. Therefore, loss reduction rate seems to be saturated for high St-number and the effect of St-number is negligible. Therefore, a certain amount of the performance improvement by using the PTE airfoil can be expected regardless of the St-number at high Re number condition without burst flow.

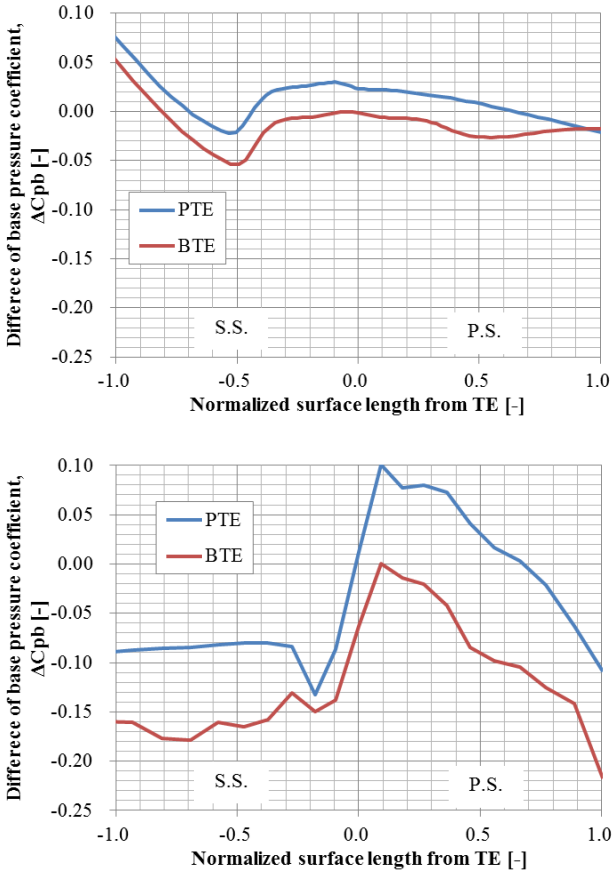

Fig. 10: Distribution of static pressure difference resulting from CFD between that at TE and at 30% *Cx* far from the TE. The pressure difference is normalized by mass averaged total pressure at 30% *Cx* far from TE for HSR

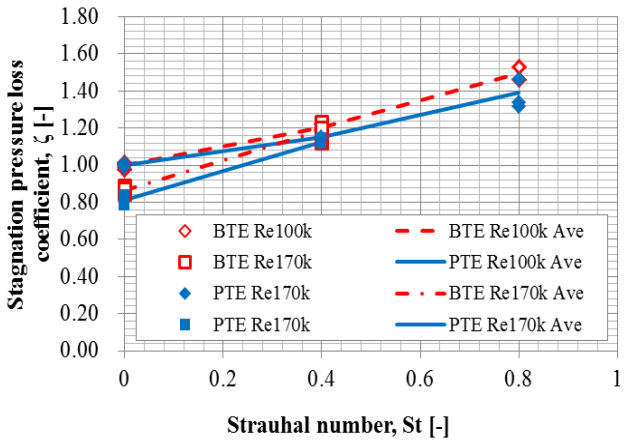

Fig. 11: Normalized total pressure loss coefficient for various St-numbers tested in low speed cascade experiment.

Effect of velocity triangle and velocity levels

One of the differences between the conditions for the HSR and that for the LSC is Mach number. Mach number at turbine exit around 50% span for HSR is over 10% larger than that for LSC. In order to extract the effects of velocity triangle and Mach number, the flow field is calculated with MISES[9]. The calculation is based on Euler equation to distinct the geometric characteristics. The isentropic Mach number distributions on the surface calculated from MISES are shown in Fig. 12. The isentropic Mach number is calculated by using turbine exit flow condition and surface pressure distribution. Note that the Mach number distributions are normalized the value at the TE on surface. As seen in Fig. 12, the position of peak Mach number is difference. The position which takes the maximum Mach number is 46%*Cx* for LSC and 70%*Cx* for HSR. Therefore the deceleration on the turbine airfoil is seen as different. However, as seen in Fig. 13, the velocity distribution on the surface of base type airfoil for HSR is similar to that for LSC. Note that the velocity distributions are also normalized by the value at the TE and the x-axis indicates the surface length from LE. The deceleration rate of base type airfoil for HSR is almost the same as that for LSC and the length of the regions between maximum values of velocity to that at TE is 5% different from the length of suction surface. Therefore the phenomena that caused at turbine decelerating region at the HSR are similar to that at the LSC. This result expects that the boundary layer development on deceleration region of the HSR is similar to that of the LSC. Moreover, it is also expected that the loss creation at the deceleration region does not change significantly. Therefore the influence of the velocity triangle and velocity levels is negligible in this paper.

Total loss reduction

In order to summarize the influence of the high speed rig on the loss reduction, the total loss contribution is considered. The total loss reduction values are shown in Table 6 by using above discussions. The total value of loss reduction of the PTE for HSR and LSC is similar to the experimental values shown in Table 3. The effect of velocity deficit significantly contributes to loss reduction. The effect of base pressure is secondary.

Table 6: The total loss reduction rate calculated by using effect of velocity deficit and base pressure

	LSC	HSR	$\Delta\zeta$
$\Delta\zeta$ of 1st term	4%	6 %	2%
$\Delta\zeta$ of 2nd term	0 %	0 %	0%
$\Delta\zeta$ of 3rd term	1 %	5%	4%
Total difference	5%	11 %	6%

CONCLUSION

First, in order to demonstrate the performance of profiled trailing edge (PTE) airfoil that developed in IHI, high speed rotational rig experiment is conducted. The high speed rotational rig simulates the running condition of low pressure turbine of modern civil aircraft engine. From the experimental results that conducted three times, the loss reduction rate by using the PTE is 9.7 % comparing with that of Base type Trailing Edge (BTE). Also the low speed cascade experiment is conducted at Iwate University and the loss reduction rate is calculated. The loss reduction rate resulting from HRS is larger than that from LSC. The results expect that PTE can be applied to modern civil aircraft engines.

Second, in order to consider the loss reduction mechanism on HSR, the Denton's loss model is used comparing with the result from LSC. From the discussion, by dividing the occurrence of loss, the loss reduction mechanism and contribution is examined. As a result the most effective influence on loss reduction is combination of base pressure and TE blockage. Moreover, loss reduction by using PTE is independent from wake passing frequency under high Reynolds number conditions.

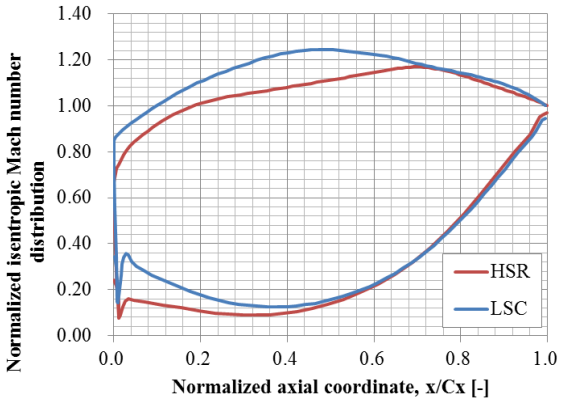

Fig. 12: Normalized isentropic Mach number distribution on normalized axial coordinate resulting from MISES Euler calculation.

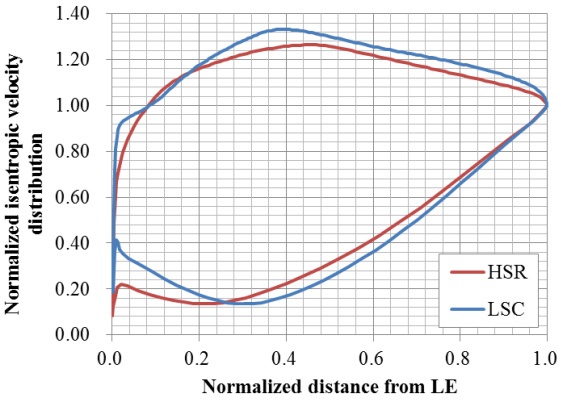

Fig. 13: Normalized isentropic velocity distribution on airfoil's surface resulting from MISES Euler calculation.

REFERENCES

[1] Denton, J. D., 1993, "loss Mechanisms in Turbomachines", *ASME Journal of Turbomachinery*, Vol. 115. No.4 pp. 621-656.

[2] Mee, D. J., Baines, N.C, Oldfield, M.L.G, Dickens, T.E., 1992, "An examination of the contributions to loss on a transonic turbine blade in cascade", *ASME Journal of turbomachinery*, Vol. 114, No. 1 pp. 155-162.

[3] Okamura, K. 2012, *Master Thesis*

[4] Funazaki, K., Okamura, K., Ebina, Y., Sato, Y., Kosugi, T., Takahashi, A., Mamada, A., 2013 "A Novel Method for Improvement of Aerodynamic performance of Highly Loaded LP Turbine Airfoils for Aeroengines", *Proceedings of ASME Turbo Expo 2013: Turbine Technical Conference and Exposition*, GT2013-94745.

[5] Lueders, H. G. 1970, "Experimental Investigation of Advanced Concepts to Increase Turbine Blade Loading", *NASA Contractor Report*

[6] Herman, W., Prust, J., Ronald, M. H., 1972, "Effect of Trailing-Edge Geometry and Thickness on the Performance of Certain Turbine Stator Blading", *NASA Technical Note*

[7] Chao, Z., Howard, H., Christoph, H., 2013, "The Effects of Trailing Edge Thickness on the Losses of Ultra-High Lift LP Turbine Blades", *Proceedings of ASME Turbo Expo 2013: Turbine Technical Conference and Exposition*, GT2013-94029.

[8] Menter, F. R., Langtry, P. B., Likki, S. R., Suzen, Y. B, Huang, P. G., Volker, S., 2006, "A Correlation Based Transition Model Using Local Variables Part 1 – Model Formulation", *Journal of turbomachinery* Vol. 128, No. 3 pp. 413-422.

[9] Drela, M., Youngren, H., 1998, "A User's Guide to MISES 2.53", Dept. of Aerounautics and Astronautics, Massachusetts Institute of Technology, 70 Vassar St, Cambridge MA 02139.